JOURNAL OF GEOPHYSICAL RESEARCH, VOL. 95, NO. C3, PAGES 2939–2952, MARCH 15, 1990

The Impact of the Wet Tropospheric Correction on the Interpretation of Altimeter-Derived Ocean Topography in the Northeast Pacific

PATRICIA A. PHOEBUS[1] AND JEFFREY D. HAWKINS

Ocean Sensing and Prediction Division, Naval Ocean Research amd Development Activity, Stennis Space Center, Mississippi

Atmospheric water vapor data derived from the special sensor microwave/imager (SSM/I) are used to make time-coincident, wet tropospheric range corrections to Geosat altimeter data in the northeast Pacific. The original and corrected sea surface height residuals along numerous tracks are examined to determine the impact of water vapor on the altimeter signal. Mesoscale feature analyses of corrected and uncorrected altimeter data are used to assess the impact of water vapor path lengthening in areas of low sea surface height variability. Results indicate that the horizontal spatial variations in the water vapor height corrections are frequently similar to true oceanographic gradients. Interpretation of altimeter data is affected in several ways. The unaccounted-for presence of atmospheric water vapor may mimic or mask the true ocean features, and even small changes in the water vapor over short spatial scales can enhance a partially obscured feature. Analyses of all Geosat tracks crossing the area of interest in September 1987 clearly illustrate that water vapor frequently contaminates the ocean topography measurements, making the water vapor adjustment critical before the altimeter data can be successfully used to locate and identify mesoscale ocean features. Furthermore, the SSM/I and Geosat data must be closely matched in both space and time, a difficult task since it takes 3.5 days to obtain global SSM/I coverage with one operational sensor. To optimize the mesoscale oceanographic application of altimeter data, a bore-sighted radiometer should be included on all altimeter spaceborne platforms.

INTRODUCTION

The U.S. Navy launched a radar altimeter aboard the Geosat platform on March 12, 1985. Its primary mission was to provide the data needed to precisely map the Earth's geoid over the oceans [*McConathy and Kilgus*, 1987]. However, because the altimeter measures the ocean topography and other parameters along its track, it also provides important and useful oceanographic data. For example, the Naval Ocean Research and Development Activity (NORDA), through the Geosat Ocean Applications Program (GOAP), used the sea surface height (SSH) data to successfully locate mesoscale fronts and eddies in the Gulf Stream region [*Lybanon and Crout*, 1987]. Nevertheless, significant mesoscale oceanographic features are found in many parts of the world. We want to determine whether or not mesoscale altimeter data analysis can be extended to areas where the SSH variability is not as pronounced.

One such area is the northeast Pacific. There are several weak fronts in this area with dynamic height perturbations of 5–15 cm over 100–300 km [*Roden and Robinson*, 1988]. NORDA is involved in an extensive northeast Pacific (NEPAC) research project coupling real-time data analysis, remote sensing, and ocean prediction and acoustic modeling efforts. Our role in this project is to determine the usefulness of remotely sensed data (both infrared imagery and altimeter data) for locating mesoscale fronts and eddies. Because the SSH gradients in this area are weak, the potential altimeter error sources are more critical. Of these, the main error that is unaccounted for is the apparent path lengthening created by the columnar atmospheric water vapor, also referred to as the vertically integrated water vapor or precipitable water (hereinafter referred to as WV). This error potentially occurs over the same length scale as mesoscale ocean features.

The presence of WV increases the time it takes the radar pulse to pass through the atmosphere to the ocean's surface and return. Since the distance to the surface is computed as a function of this transit time, when WV is present the ocean surface appears farther away than it actually is, resulting in a SSH estimate that is too low. Furthermore, if sharp horizontal gradients are present in the WV distribution, the apparent shape of the ocean's surface along the altimeter track may be significantly altered, and WV gradients may be mistakenly interpreted as actual mesoscale ocean features. In contrast, if abrupt WV changes occur at approximately the same location as the ocean features of interest, then the WV gradients may counteract the slope of the ocean topography, thereby masking or obscuring the true feature's signal. Early results from a few selected cases suggest that the presence of WV may seriously hinder the application of altimeter data for mesoscale oceanography in areas of relatively weak ocean signals [*Phoebus and Hawkins*, 1988]. Thus the purpose of this paper is to look in more detail at high-resolution WV data in the NEPAC region and determine how the WV alters the true mesoscale ocean signal and affects detection and interpretation of ocean features.

Columnar water vapor data have been provided by satellite passive microwave sensors since the launch of Nimbus 5 in 1972. Measurements from the electrically scanning microwave radiometer provided information with an estimated accuracy of 4.2 kg m^{-2} for the derived WV [*Staelin et al.*, 1976]. WV data from the scanning multichannel microwave radiometer (SMMR), launched on Nimbus 7 in 1978, provided observations at a horizontal resolution of 50 km with a swath width of 800 km. Advancement in algorithm development and sensor performance resulted in rms errors of

[1]Now at Naval Oceanographic and Atmospheric Research Laboratory, Atmospheric Directorate, Monterey, California.

Paper number 89JC03093.

2.1 kg m^{-2} kg m^{-2} when compared with independent radiosonde observations [*Chang et al.*, 1984]. A SMMR was also flown on board Seasat, which during its short life (3 months) provided the only same-track measurements of ocean topography and WV data. Finally, the special sensor microwave/imager (SSM/I) on board the polar-orbiting Defense Meteorological Satellite Program (DMSP) platform has provided WV measurements at 25-km resolution within 1394-km swaths since June 1987. This is by far the most comprehensive spatial coverage of the global atmospheric moisture data available to date. The accuracy of these data is estimated at 2.4 kg m^{-2} globally [*Alishouse et al.*, 1990]. While this accuracy is slightly worse than that specified for the SSMR, the SSM/I has been in orbit a much shorter time and thus has a smaller data base from which to determine the accuracy of the observations.

Many studies have used remotely sensed WV data to describe atmospheric moisture fields over large space and time scales [*Chang et al.*, 1980; *Chelton et al.*, 1981; *Njoku and Swanson*, 1983; *Short and Prabhakara*, 1984]. While these types of studies are useful for climatic and modeling applications, they do not address our specific needs. Only a few efforts have been made to analyze WV using the temporal and spatial scales appropriate for oceanographic mesoscale applications. *Askne et al.* [1986] used atmospheric modeling techniques to estimate the altimeter path delay due to WV. *Hawkins and Smith* [1986] used Seasat SMMR data to show that the change in the altimeter path length due to WV alone can be 20–40% as large as the Gulf Stream front and eddy signals and that these gradients can occur over the same time and space scales as the features themselves. More recently, *Monaldo* [this issue] extensively analyzed Seasat SMMR WV gradients over spatial scales from 100 to 300 km for much of the world's oceans, while *Bisagni* [1989] used a limited data set to compare model-predicted WV [after *Saastamoinen*, 1972] with data from rawinsondes in the area near 69°W, 27°N at spatial scales up to 500 km. Both Monaldo and Bisagni concluded from their statistical studies that WV height corrections do not play a major role in the interpretation of mesoscale ocean features on their scales of interest, primarily for signals of at least 10 cm per 100 km. Furthermore, neither of these studies rigorously attempted to relate the presence of atmospheric frontal systems to the WV gradients.

Our study takes a somewhat different approach by looking at the impact of actual wet tropospheric corrections made to real altimeter SSH residuals. We pay particular attention to the relationship between the atmospheric fronts and the associated WV fields, focusing on changes in the oceanographic signal that are as small as 5 cm per 100 km. Since our interest is in the near-real-time location of mesoscale ocean features, our primary concern is how the wet tropospheric correction alters the interpretation of individual tracks. In this regard, our study is unique, which may explain why our conclusions differ from previous studies.

To satisfy the need for high-resolution WV data, we compute precipitable water from the SSM/I brightness temperatures, which provides a nearly instantaneous picture of the WV variability within an individual swath. The WV data are objectively analyzed along individual Geosat tracks and are used to make realistic wet tropospheric range corrections to the altimeter SSH measurements. Evaluation of the WV corrections along each track allows us to identify large WV gradients, classify them according to their magnitude and range, and determine the frequency with which they occur on the same time and space scales as the ocean feature of interest. In addition, by analyzing the SSH data both before and after the wet tropospheric correction is applied, we can quantify how frequently the presence of WV changed the physical interpretation of the altimeter data. The data sources, analysis methods, results, and conclusions are presented in the following sections.

SATELLITE DATA SOURCES

Altimeter Data

The March 1985 Geosat launch represented the first U.S. altimeter in space since the short-lived Seasat mission. Numerous Seasat studies had looked into various aspects of oceanographic mesoscale and monthly signals and variability [*Cheney*, 1982; *Bernstein et al.*, 1982; *Menard*, 1983; *Thompson et al.*, 1983], but they were limited due to the 3-month data base. Geosat (similar in most respects to the Seasat altimeter) thus provided the extended time series required to determine the long-term basin-scale oceanic changes. More importantly for this study, it provided a continuous ground track of reliable SSH measurements that could be used to help locate ocean fronts and eddies. Unfortunately, Geosat is a single-sensor satellite that provides measurements of ocean topography only and, unlike Seasat, does not produce coincident WV measurements.

The GOAP at NORDA was the first effort to routinely process and analyze altimeter data in real time and follow up the natural evolution begun with earlier Seasat Gulf Stream work [*Cheney*, 1982]. Figure 1*a* exhibits the 17-day repeat track spacing available as part of the Geosat Exact Repeat Mission. Altimeter data along these tracks were used in the GOAP study in conjunction with satellite infrared imagery and available in situ observations to extract Gulf Stream front and eddy information [*Lybanon and Crout*, 1987]. Weekly maps of ocean frontal features were generated by extracting the 30- to 150-cm signals associated with warm- and cold-core rings and the north and south wall of the Gulf Stream.

Error sources (Table 1 [after *Lybanon and Crout*, 1987]) were not normally a significant hurdle to overcome, since Gulf Stream ocean signals were dominant in magnitude within the mesoscale spatial domains. Some problems were noted with ring detection [*Hawkins and Smith*, 1986], particularly older cold-core rings that maintained faint signals and rings that were sampled near their edges rather than across their centers. However, sufficient corrections were generally made to permit accurate interpretation of the data, especially in this major western boundary current regime. However, the main purpose of this paper is to report the impact of wet tropospheric corrections on SSH values in a region of very weak ocean frontal signatures, particularly, for the NEPAC area along the Geosat tracks shown in Figure 1*b*. Since it is generally accepted that the altimeter SSH measurements exhibit an engineering noise level near 3 cm [*Sailor and LeSchack*, 1987], it should be possible to detect ocean features that exhibit weaker signals than those in western boundary currents, particularly if the correction for the WV can be made.

The Geosat data are telemetered to the Earth-receiving

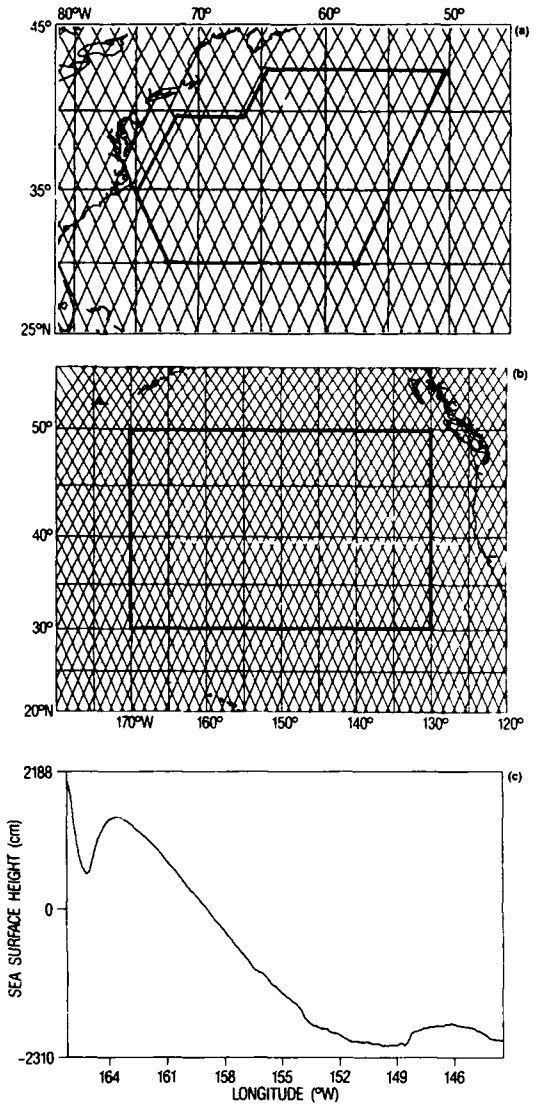

Fig. 1. Geosat 17-day repeat tracks from the Exact Repeat Mission. (*a*) The GOAP research area is outlined in the northwest Atlantic. (*b*) Geosat tracks in the NEPAC research area. (*c*) Mean surface profile computed along Geosat track A58.

station at the Applied Physics Laboratory Johns Hopkins University, twice daily. Minor processing is done before the data records are transmitted to NORDA and the Naval Oceanographic Office at Stennis Space Center. Minimal processing produces ocean surface wind speed, significant wave height, and sea ice products that are relayed to the Fleet Numerical Oceanography Center in Monterey, California. More accurate ephemeris data from the Navy Astronautics Group arrive within 24 hours and are then incorporated to help produce SSH height values. The mean surface along a repeat track is determined by averaging data from multiple passes along the same track (usually over a period of at least 1 year). The mean surface is then subtracted from the individual tracks to form SSH residuals. Corrections are also made for orbit errors, and the tilt and bias are removed from the SSH residual data before they are used for mesoscale interpretation.

Note that the computation of residuals by subtracting a mean surface from the altimeter data removes not only the geoid but also the mean circulation. This does present the possibility that the residual circulation signal is somewhat reduced if it coincides with the mean circulation in the area. How often this actually occurs, we cannot say. However, this method for computing the residuals seems to be the least worrisome. If two collinear tracks were differenced, then we would have to be concerned about the effect of WV path lengthening on both tracks; if a synthetic geoid were used, then we would need to address the errors in the model used to produce the geoid. An example of the mean surface in the NEPAC area is shown in Figure 1*c*. Note that the scale of the gradient associated with this mean surface is several orders of magnitude larger than that used to distinguish ocean fronts in this area.

TABLE 1. Geosat Measurement Uncertainty

Error Source	Uncertainty (σ) Baseline Mission, cm	Uncertainty (σ) Extended Mission, cm	Wavelength of Error, km
	Altimeter		
Instrument noise	2.0	2.0	
Bias drift	2.0	2.0	many days
Time tag	0.2	0.2	20,000
Tracker bias	2.0	2.0	200–1,000
	Media		
Electromagnetic bias	2.0	2.0	200–1,000
Skewness	1.0	1.0	200–1,000
Troposphere (dry)	0.7	0.7	1,000
Troposphere (wet)	6.0	3.0	200
Ionosphere	4.0	4.0	>1,000
	Orbit		
Gravity	80.0	50.0	>10,000
GM	2.0	2.0	10,000
Atmospheric drag	10.0	10.0	10,000
Troposphere	1.0	1.0	10,000
Solar radiation pressure	10.0	5.0	10,000
Earth albedo	2.0	1.0	10,000
Earth or ocean tides	1.0	1.0	10,000
Station or spacecraft clocks	10.0	10.0	10,000
Higher-order ionosphere	5.0	5.0	10,000
Root Sum of Squares	83.0	54.0	

Major assumptions for the baseline mission are (1) TRANET tracking system, 40 stations; (2) TRANET ground station oscillators perform to specifications; (3) altimeter data averaged over 1 s; (4) $H_{1/3}$ = 2 m, wave skewness = 0.1; (5) limited tuning of gravity field with Geosat TRANET data; (6) 800-kilometer altitude; (7) No anomalous data and no rain; (8) ±3 mbar surface pressure from weather charts; and (9) 100-μs spacecraft clock. Major assumptions for the extended mission are the same as for the baseline mission, but with (1) improved gravity, station location, and drag models based on Geosat tracking and (2) use of water vapor correction from SSM/I.

Water Vapor Data

The SSM/I is a seven-channel, four-frequency (19, 22, 37, and 85 GHz), passive microwave sensor flown aboard the polar-orbiting DMSP platform [*Hollinger*, 1989]. The 1394-km swath (roughly twice that of preceding sensors) and high-resolution spot sizes (Table 2) indicate several advantages this sensor has over the SMMR flown on Seasat and Nimbus 7. However, even the large SSM/I scan requires 3.5 days to fully cover the global oceans, thus leaving data gaps over shorter time frames.

TABLE 2. SSM/I Channel Spatial Resolutions

Channel Frequency, GHz	Polarization	Effective Field of View, km	Scene Station Spacing, km
19.350	vertical	55.3	25.0
	horizontal	55.1	25.0
22.235	vertical	48.6	25.0
37.000	vertical	32.2	25.0
	horizontal	32.7	25.0
85.500	vertical	14.8	12.5
	horizontal	14.8	12.5

The SSM/I can measure many atmospheric and oceanographic environmental parameters: sea ice (edge, concentration, and distinction between first-year and multiyear ice), WV, surface wind speed, cloud liquid water, rain rate, etc. The SSM/I channels are particularly well suited to retrieve total columnar or vertically integrated WV as noted by the long heritage of similar space sensors. The SSM/I's superior 25-km resolution should permit the best depiction yet of the horizontal variations in the WV distribution associated with atmospheric frontal systems.

Past efforts to validate satellite-derived WV retrievals have focused on the use of ocean weather ship and island radiosondes [*Taylor et al.*, 1981; *Lipes*, 1982; *Chang et al.*, 1984; *Tapley et al.*, 1984]. This data base is typically small and requires special efforts to gather enough temporal and spatial matchups to represent a significant statistical sample. Most studies include less than 100 radiosonde versus satellite sensor comparisons, but they typically indicate that the quality of the remotely sensed WV closely matches that of the radiosonde values. The accuracy of the radiosonde measurements is of the order of 1.7 kg m^{-2} [*Taylor et al.*, 1981].

Progress in sensor and algorithm development is shown by improved performance over the last 12 years and is reflected in the high- quality DMSP SSM/I retrievals. As stated, the latest findings of *Alishouse et al.* [1990] show that a global algorithm now provides WV to an accuracy of 2.4 kg m^{-2}. Similar findings were made by F. Wentz (personal communication, 1989), who has processed over 1 year of SSM/I data for NASA projects and computed the accuracy of the WV values as approximately 3.0 kg m^{-2}.

The Wentz data are incorporated in our study, since they represent the first lengthy SSM/I data set available to test the capabilities of this sensor's wide swath and high spatial resolution in defining WV gradients that may adversely impact altimeter SSH studies. The brightness temperatures at 19 and 22 GHz were combined to derive the precipitable water. These WV measurements (in kilograms per square meter) were converted to altimeter wet tropospheric corrections by multiplying by the scalar quantity, 0.00636 m [*Tapley et al.*, 1982]. Further refinements of this conversion factor by comparison with a larger radiosonde data set indicated little change in the value selected, especially in mid-latitudes [*Tapley et al.*, 1984]. Thus the individual SSM/I measurements of the precipitable water, ranging from under 10 kg m^{-2} to over 60 kg m^{-2}, were changed into altimeter path length corrections expressed in centimeters, extending from near 0 to almost 40 cm.

There is only a small error inherent in this method.

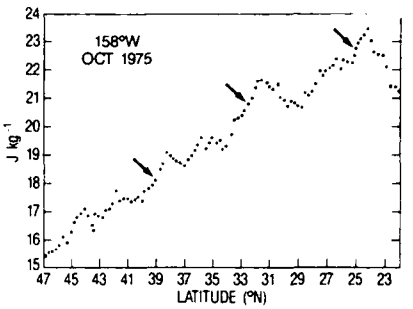

Fig. 2. Sea surface dynamic height perturbations (relative to 1500 dbar) from north to south along 158°W, derived from in situ cruise data in October 1975 [after *Roden*, 1977]. A 1 J kg^{-1} perturbation is equivalent to 10 cm of sea surface height. Arrows indicate mesoscale ocean features.

Multiplying the rms WV error (3.0 kg m^{-2}) by 0.00636 generates a SSH correction error near 1.9 cm. This measurement inaccuracy is well within the tolerance needed to map the 0- to 40-cm WV correction within the NEPAC grid sector. Also, since the conversion factor is a constant, a direct linear relationship exists between the wet tropospheric correction gradients and the actual gradients in the atmospheric WV.

Data Analysis

The NEPAC area is a suitable location for testing the limits on the use of altimeter data for detecting mesoscale ocean features. Figure 2, an example of the SSH variability in this area, was derived from in situ cruise data [*Roden*, 1977]. Several fronts can be identified by the rather sharp increase in the height perturbations (from north to south) of less than 10 to near 30 cm over 100–200 km. Thus the SSH variability here is small compared with that found near the Gulf Stream, which typically contains signals of 50–150 cm over the same distance.

To determine how WV path lengthening affected the usefulness of the altimeter data, we obtained SSM/I WV data for July–September 1987 and also for portions of February 1988. This data set provided observations from summer, early fall, and winter. Several cases were selected for study by using the sea level–pressure surface analyses from the National Meteorological Center (NMC) to identify days when a strong atmospheric front was present in the area of interest. The largest WV gradients are normally associated with such atmospheric frontal systems [*McMurdie and Katsaros*, 1985], so the selected days provided an initial look at potential worst case scenarios.

After converting the WV data to WV corrections, the corrections were objectively analyzed to produce a uniformly gridded, two-dimensional field at 1.0° resolution. The area encompasses 30° to 50°N and from 130° to 170°W. This area coincides with the area for which the mean surface has been computed. A simple objective analysis scheme was used for the interpolation, where the weight of each data point was first determined, following *Cressman* [1959], from

$$w_i = \frac{R^2 - d_i^2}{R^2 + d_i^2} \tag{1}$$

where R is the specified data search radius, d_i is the distance of each data point from the analysis grid point, and w_i is the

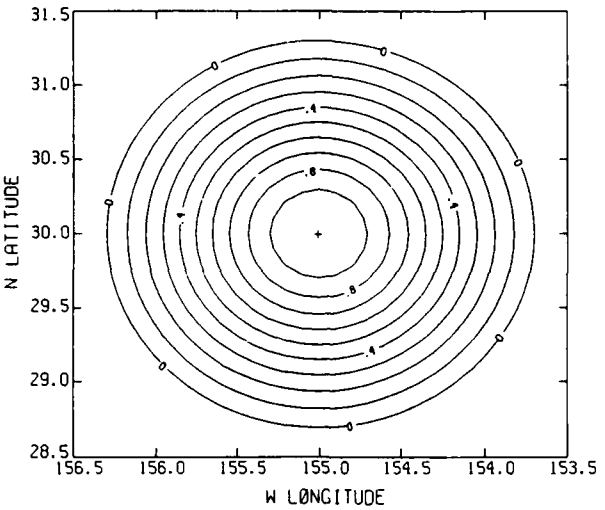

Fig. 3. Weighting function chosen for the data analysis scheme $w = (R^2 - D^2)/(R^2 + D^2)$. Contours represent the weight w computed as a function of distance D from a sample analysis point at 30°N, 155°W, given a search radius R of 1.3°.

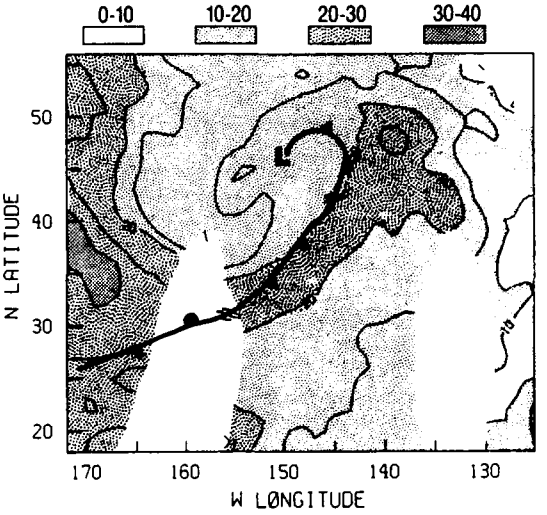

Fig. 4. Water vapor (WV) correction field analyzed using SSM/I vapor data from 0200 UT to 1600 UT, August 1, 1987. Contours are every 5 cm. Darker shades represent higher WV content. The atmospheric frontal position is valid at 0000 UT on the same day.

relative weight assigned to each data point. The final weights W_i are computed by normalizing the relative weights:

$$W_i = \frac{w_i}{\sum_{i=1}^{N} w_i} \tag{2}$$

where N is the number of data points within a distance R of the grid point. The analyzed WV correction V at the grid point is then determined from the linear combination

$$V = \sum_{i=1}^{N} W_i v_i \tag{3}$$

where v_i is the computed correction and W_i is its associated weight computed in (2).

Newer, more sophisticated analysis techniques, such as optimum interpolation, are difficult to apply to this problem. Use of optimum interpolation, for example, requires knowledge of the proper correlation function and spatial correlation scales of the target field. Although meteorologists have used this technique for years to analyze atmospheric moisture (in the form of relative or specific humidity), they use wind speed and wind direction fields to specify the necessary statistical functions [*DiMego*, 1989]. Since access to this kind of information was not readily available, we chose the simple scheme described above, which is basically a nonlinear inverse distance-weighting scheme (Figure 3).

As long as R is chosen intelligently, this type of objective scheme will produce interpolated fields that are smoother than the original observations. For the two-dimensional analysis, R was selected to be 1.3 times the grid increment of 1.0°. This value allows sufficient overlap of the data search areas at adjacent grid points and thus does not induce subgrid-scale features into the data. Rather than simply extrapolate the nearest one or two measurements to the given location, many observations are incorporated into the analytical solution. Thus the amount of random noise is reduced, and the resulting fields are representative of the grid scale being analyzed.

To qualitatively validate the analysis scheme, the two-dimensional WV correction fields were plotted and compared with the NMC surface atmospheric frontal positions closest in time to the SSM/I data. In all cases, agreement between the maximum WV gradient locations and the positions of the atmospheric fronts was extremely close. An example (Figure 4) shows a band of moist air along the cold front, which wraps around and behind the low pressure center and which contrasts sharply with the cold, dry air behind the front. This pattern is exactly what would be expected, given *Bjerknes'* [1919] classical cyclone model definition. Similar patterns have also been shown quite clearly in studies by *McMurdie and Katsaros* [1985], *Katsaros and Lewis* [1986], and *McMurdie et al.* [1987]. This relationship between the atmospheric systems and the maximum WV content and variability was observed repeatedly in our data. Thus we are confident that the analyzed WV corrections are indicative of the real-time synoptic atmospheric moisture patterns.

Within a given 24-hour period, three ascending and three descending SSM/I swaths passed either completely or partially through the NEPAC region. While the exact times vary somewhat, the data provided by descending passes were from around 0200 UT to 0700 UT and the ascending passes were between 1400 UT and 1900 UT (Figures 5*a* and 5*b*). The time separation of the swaths is approximately 1.5 hours. As illustrated, there are data coverage gaps as far north as 54° N. Although the analysis scheme partially fills in the data-void areas, it cannot extrapolate information any farther than the specified search radius, which is approximately 145 km. Thus in some cases, data from both the ascending and descending swaths were blended by the analysis, with no change in the data weights as a function of time. This procedure improves the amount of coverage in the area (Figure 5*c*) but can create other problems, particularly if the atmospheric system is rapidly moving.

Figure 5 demonstrates significant differences between the ascending and descending swaths analyzed separately and the sets blended together. The most notable difference is in the position and shape of the maximum WV correction

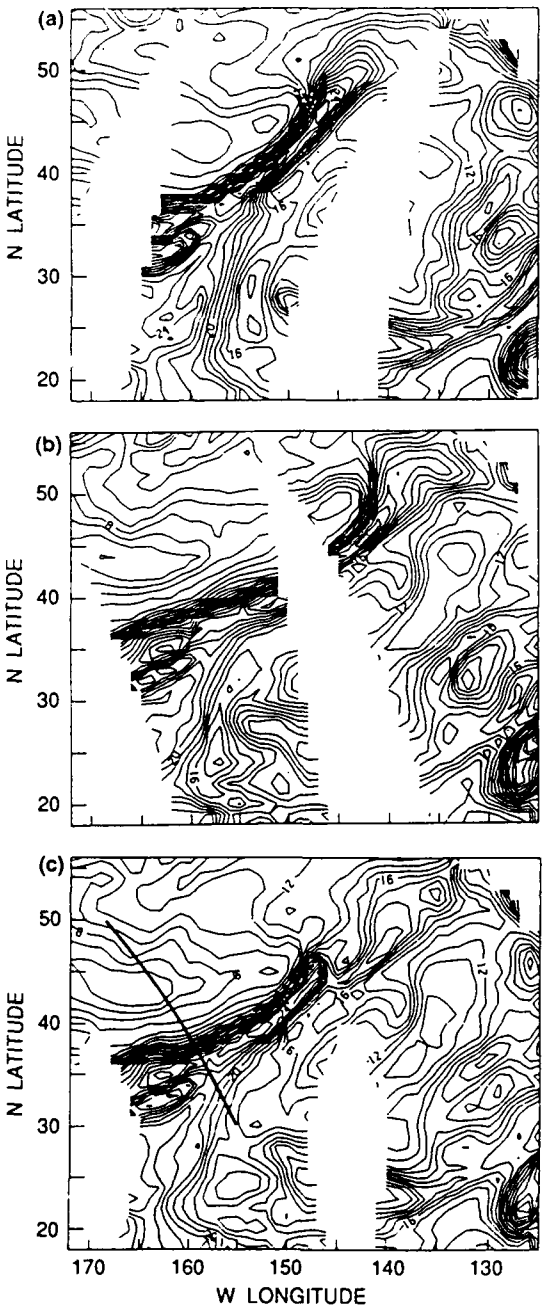

Fig. 5. WV correction fields analyzed using SSM/I data on July 12, 1987. Contours are every 1 cm. (*a*) Descending swaths only, from 0300 to 0700 UT; (*b*) ascending swaths only, from 1400 to 1800 UT; (*c*) descending and ascending swaths blended together. The 1900 UT Geosat track is shown crossing the strong gradient in the field.

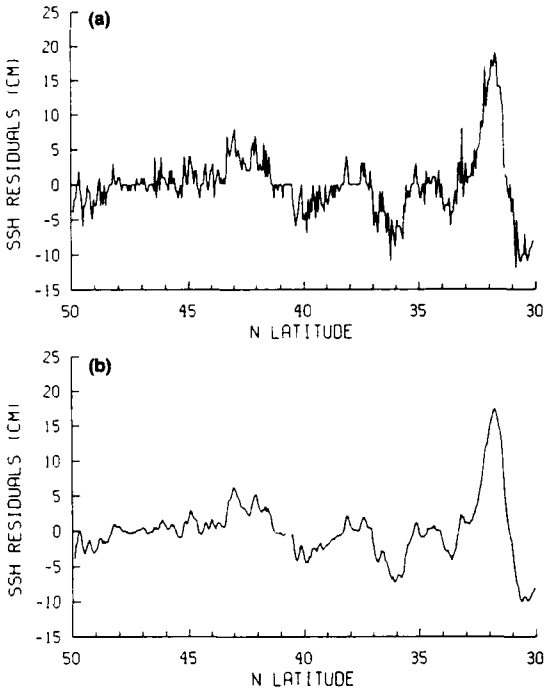

Fig. 6. Altimeter sea surface height (SSH) residuals along the 1900 UT Geosat track on August 1, 1987. (*a*) Original unsmoothed SSH data. (*b*) Smoothed SSH data.

gradient as the sharp gradient associated with the cold front around 150°W, 45°N, shifted southeastward as the front advanced to the east (Figures 5*a* and 5*b*). The northern portion of the front near the low pressure center moved more rapidly than the trailing end of the front. As a result, the northern edge of the blended WV correction field introduced a false gradient around 148°W, 45°N, while oversmoothing the gradient north of this point (Figure 5*c*). This problem will be addressed more thoroughly in the next section.

The original SSM/I data, not the previously analyzed two-dimensional field, were used to compute the WV corrections along a given altimeter track. The same analysis technique was applied, but the analysis points in this case were positioned at exactly the same location as each altimeter footprint. The average distance between altimeter points is approximately 7 km, while the SSM/I data has a resolution of 25 km; therefore a search radius considerably larger than the separation of the analysis points was necessary. A 50-km search radius was selected to allow several SSM/I measurements to be included in the analysis at any one point, while still showing more detail in the one-dimensional WV correction curve than in the two- dimensional analysis.

Before the altimeter SSH residuals were corrected for WV, they were smoothed using a five-point filter (Figure 6). Thus each measurement was replaced by the average of the original value and the four closest measurements. This smoothing reduced the noise in the signal sufficiently without removing the features of interest. The wet tropospheric adjustment was then made by adding the analyzed path length correction at each footprint to the smoothed SSH value. In each case, the WV correction curve analyzed along the track was plotted in conjunction with the original and the corrected SSH data, allowing an easy visual comparison between the features in each representation.

The SSH data along a given track were examined to determine if the observed signal indicated the presence of an ocean front. This type of analysis is performed routinely as part of the NEPAC project, using the techniques described by *Lybanon and Crout* [1987]. Both infrared sea surface temperature data and altimeter data were used. Ongoing analyses have demonstrated that NEPAC fronts are characterized by an increase of 5–20 cm in the altimeter SSH residual (looking from north to south) over spatial scales of 100–200 km. Thus corrected and uncorrected SSH data for

each track were contrasted to identify the changes in the strength and location of the apparent ocean features. The results will be discussed in the next section.

INTERPRETATION OF RESULTS

The WV corrections plotted along the altimeter tracks generally fell into one of three categories. Some of the correction curves were relatively constant, exhibiting little change in WV along the track (Figure 7*c*). This was much more common in descending than ascending tracks (8 out of 11 flat tracks were descending), since the descending tracks more often parallel rather than cross the typical southwest to northeast orientation of the atmospheric cold fronts (Figures 7*a* and 7*b*). Other correction curves showed only broad gradients, where the change in WV was substantial but occurred over large spatial scales (Figure 8). This type of WV field did not affect the appearance of an individual ocean feature within the altimeter data under most circumstances. The third category includes those cases where the WV fluctuations are large, that is, where the analyzed WV correction increases or decreases rapidly over small spatial scales.

Here we defined a significant WV gradient as one where the wet tropospheric correction changed by at least 2.5 cm over 0.5° latitude, which is approximately 5 cm per 100 km. This gradient is comparable to the weak ocean frontal gradients that have been observed in the NEPAC region. We have also seen comparable gradients in the WV correction fields in numerous cases, which has several implications.

First, an apparent mesoscale ocean feature in the original altimeter SSH data may actually be due to abrupt changes in the WV field. An example is shown in Figure 9, where the front seen at 44°N in the original data is absent in the corrected altimeter data (Figure 9*b*). This apparent feature was due to the large WV gradients at 44°N (Figure 9*a*). Second, the WV may conceal the true ocean signal enough to completely mask the ocean front or eddy (see Figure 10). Note the front present at 39°–40°N in the corrected data that was not manifested in the original SSH data (Figure 10*b*). The front was suppressed by the presence of a strong WV gradient at the same location (Figure 10*a*). Third, the presence of WV may suppress the signal by a few centimeters, making it difficult to positively identify a feature. In the original altimeter data shown in Figure 11*b*, there is a possible front at 41°N. Once the wet tropospheric correction (Figure 11*a*) is applied to the data, this feature is more clearly identifiable.

As was already mentioned, one concern was the time difference between the altimeter measurements and the SSM/I data used to make the height correction. Since the largest WV gradients are associated with the atmospheric frontal system, the location of these gradients can be expected to change. Since the atmospheric fronts often move rapidly through this area, at speeds up to 40 km h^{-1}, there may be little continuity between the ascending and descending SSM/I passes (Figure 5). Furthermore, the WV field will undergo modification as the atmospheric system develops or ages [*McMurdie and Katsaros*, 1985]. Thus in most cases, the ascending swaths were analyzed separately from the descending swaths, and the resulting two-dimensional fields were compared with the correction field produced by blending both sets of swaths. The same altimeter track was also corrected using these different combinations of analyzed SSM/I data.

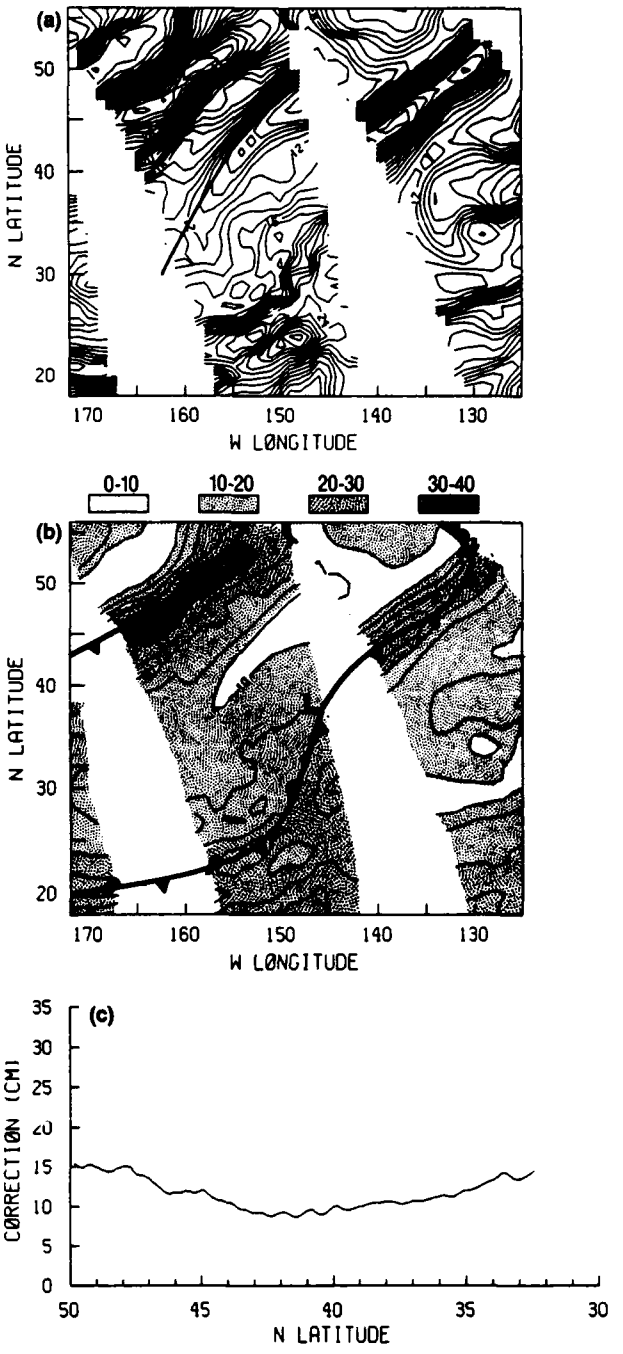

Fig. 7. WV corrections analyzed using SSM/I data on September 1, 1987. (*a*) Two-dimensional field, contoured at 1-cm intervals, with position of 2100 UT Geosat track shown. (*b*) Two-dimensional field, contoured and shaded at 5-cm intervals, showing the 1800 UT position of the atmospheric frontal systems. (*c*) One-dimensional correction curve analyzed along the 2100 UT Geosat track, using SSM/I data between 1600 and 1700 UT on the same day.

When the atmospheric fronts were either stationary or slowly moving, the 24-hour blended field closely resembled the two-dimensional fields produced from the different passes (Figures 12*a*, 12*b*, and 12*c*). In such cases, objectively combining both the ascending and descending swaths provided better data coverage, left fewer gaps in the cor-

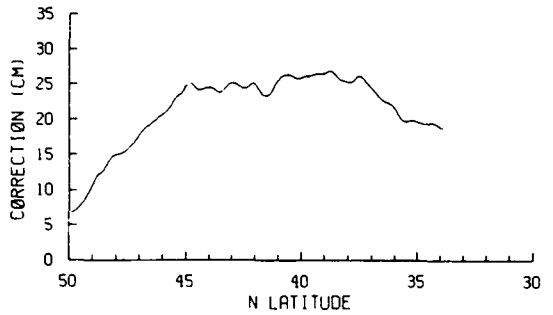

Fig. 8. WV corrections, in centimeters analyzed along the 0600 UT Geosat track on September 12, 1987, using SSM/I data between 0400 and 0500 UT.

rected altimeter data, and had little effect on the interpretation of the mesoscale features present. However, if the weather systems move rapidly or change characteristics, as was the case on September 8–9, 1987 (Figures 13*a*–13*d*), then the blending of WV data from multiple passes becomes highly questionable.

For example, the bottom curve in Figure 14*c* shows the original altimeter data measured along a track at 0700 UT on September 8 (Figure 14*a*). The top curve in Figure 14*c* represents the SSH, where the wet tropospheric correction was made using SSM/I data (Figure 14*b*) taken between 0400 UT and 0500 UT on the same day, almost coincident with the altimeter data. The broad, depressed area between 48°N and 42°N is not present in the corrected data, nor is the apparent front at 42°N. The broad depression in the SSH data was due

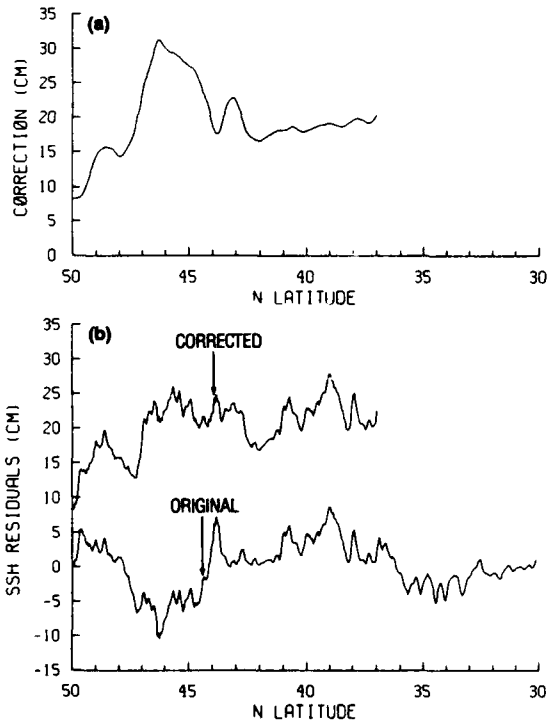

Fig. 9. WV correction applied to the 0700 UT Geosat track on September 9, 1987. (*a*) WV corrections (in centimeters) analyzed along the track using SSM/I data between 0500 UT and 0600 UT. (*b*) Altimeter SSH residuals, in centimeters, before and after the WV correction is made. Notice how the WV mimics an ocean feature at 44°N.

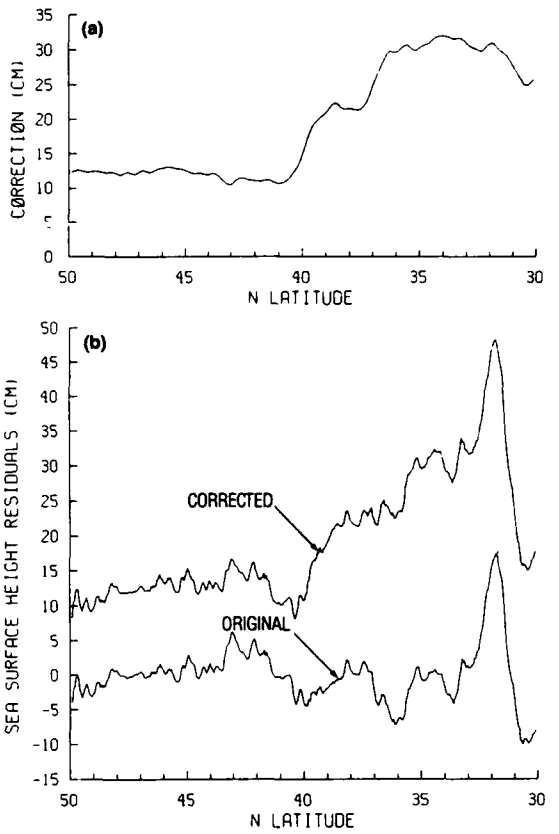

Fig. 10. WV correction applied to the 1900 UT Geosat track on August 1, 1987 (position plotted in Figure 12*c*). (*a*) WV corrections (in centimeters) analyzed along the track using SSM/I data between 0500 and 1200 UT. (*b*) Altimeter SSH residuals (in centimeters) before and after the WV correction is made. Notice how the WV masks an ocean feature at 39°N.

entirely to the band of moisture that was present along the stationary front (Figure 13*a*). The corrected data show an enhanced feature at 40.5°N, while the apparent feature at 42°N is greatly suppressed.

The same track was corrected using the SSM/I WV data sampled between 0400 UT and 0500 UT on the next day. By this time, the broad band of moisture had narrowed considerably (Figure 15*a*), and the maximum WV gradient had moved southeastward as the next cold front approached from the northwest (Figure 13*c*). Thus the peak in the WV correction along the track has both narrowed and shifted (Figures 15*b* and 14*b*). The resulting SSH data corrected with the September 9 WV data (Figure 15*c*) show significant differences from those corrected using near-real-time data. In fact, the wet tropospheric correction induced a strong signal between 43°N and 45°N. This feature is not present in the near-real-time correction (Figure 14*c*). Thus it is a false signature due entirely to the use of nonsynoptic WV data to make the wet tropospheric range correction.

These examples clearly indicate that the error in the altimeter signal due to the presence of WV is potentially a serious problem affecting the detection and interpretation of NEPAC mesoscale fronts. To determine the frequency of the problem, the data were analyzed for September 1987, at the transition from summer to fall. During this time, the contrasts between the cold, dry air masses and the warmer, moist air masses in the mid-latitudes are very strong. Thus

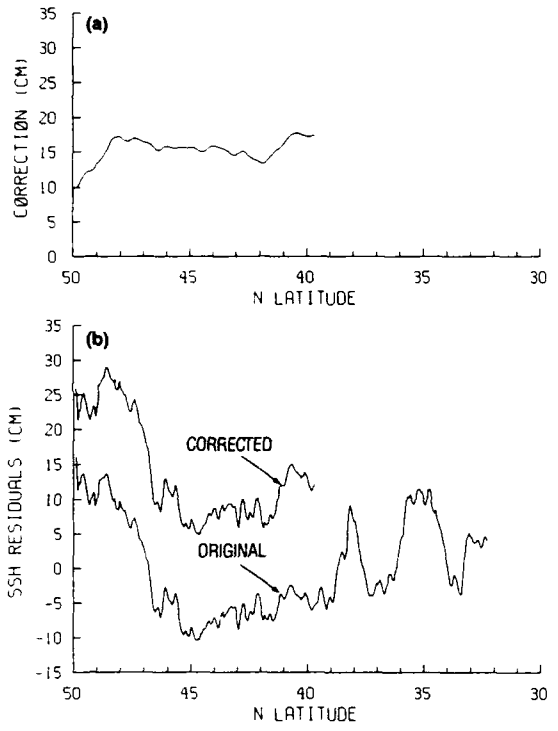

Fig. 11. WV correction applied to the 2200 UT Geosat track on September 17, 1987. (*a*) WV corrections (in centimeters) analyzed along the track using SSM/I data between 0900 UT and 1600 UT. (*b*) Altimeter SSH residuals (centimeters) before and after the WV correction is made. Notice how the WV correction enhances an ocean feature at 41°N.

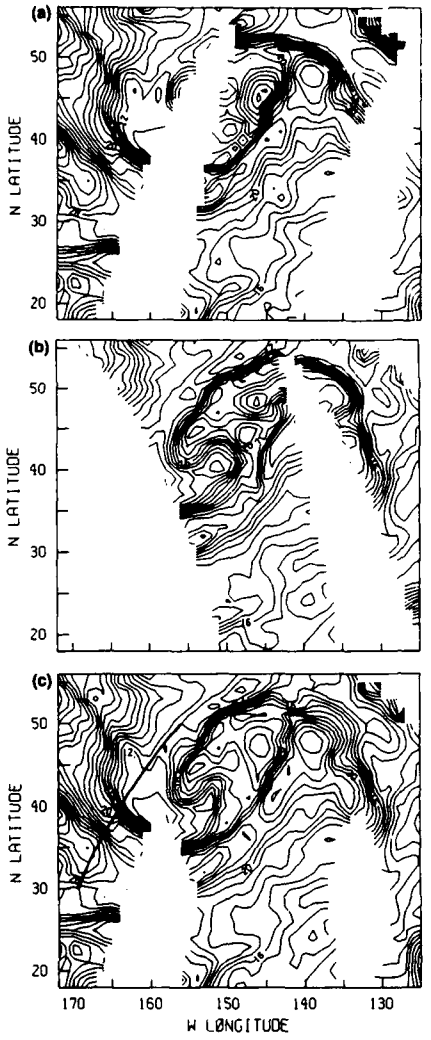

Fig. 12. WV correction fields analyzed using SSM/I data on August 1, 1987. Contours are every 1 cm. (*a*) Descending swaths only, from 0200 to 0700 UT; (*b*) ascending swaths only, from 1400 to 1800 UT; (*c*) descending and ascending swaths blended together. The position of the 1900 UT Geosat track is shown crossing the strong gradient in the field. (See Figure 10 for correction of track).

we expected that large WV gradients would accompany the meteorological systems. Furthermore, we noted that the surface pressure analyses revealed at least one atmospheric front within the NEPAC grid every day of the month. Once again, the positions of these fronts were compared with the objectively analyzed, two-dimensional, WV correction fields, and the atmospheric systems were consistently associated with the largest WV correction gradients.

Geosat tracks that passed through the NEPAC grid area during September 1987 were processed, and the SSM/I WV data were used to make the wet tropospheric correction. On the basis of visual inspection, each track was classified according to the strength of the maximum WV correction gradient along the track. Three general categories were defined: correction curves with flat gradients, broad gradients, and significantly strong gradients. The last category was further divided into three classes, representing the magnitude of the change computed in reference to 1.0° latitude (roughly 100 km). These classes were 5.0–10.0 cm, 10.0–20.0 cm, and greater than 20.0 cm. Thus each track was assigned to one of five categories. The results are shown in Figure 16. Note that of the 65 tracks processed in September, almost 75% of the tracks were associated with WV correction gradients defined as strong enough in strength to warrant concern.

This analysis differs from that made by *Monaldo* [this issue] because we studied the WV correction curve for each track and selected the endpoints over which the more abrupt changes were observed. The wet tropospheric correction gradient was initially computed over this selected distance. Each measured gradient was subsequently converted to a magnitude relative to 100 km for comparison purposes. Monaldo arbitrarily divided the tracks into fixed increments of 100–1000 km and computed the gradients over those fixed intervals. It is unlikely that this technique would capture the true WV gradient strengths, since the gradients of interest could easily extend across the fixed endpoints or fall completely in between them. Furthermore, Monaldo based his conclusions on altimeter signals that were stronger than 10 cm per 100 km, but gradients of 5 cm per 100 km may be important in some areas.

Our study identified the potentially significant gradients in each correction curve: 128 measured gradients in the 65 tracks. When classified according to strength, 76% of the gradients were in the 5.0–10.0 cm per 100 km range, with 23% in the 10.0–20.0 cm per 100 km range (Figure 17). Only two gradients exhibited signatures stronger than 20.0 cm relative to 100 km. In addition to computing the gradients relative to 100 km, the gradients in each class were grouped

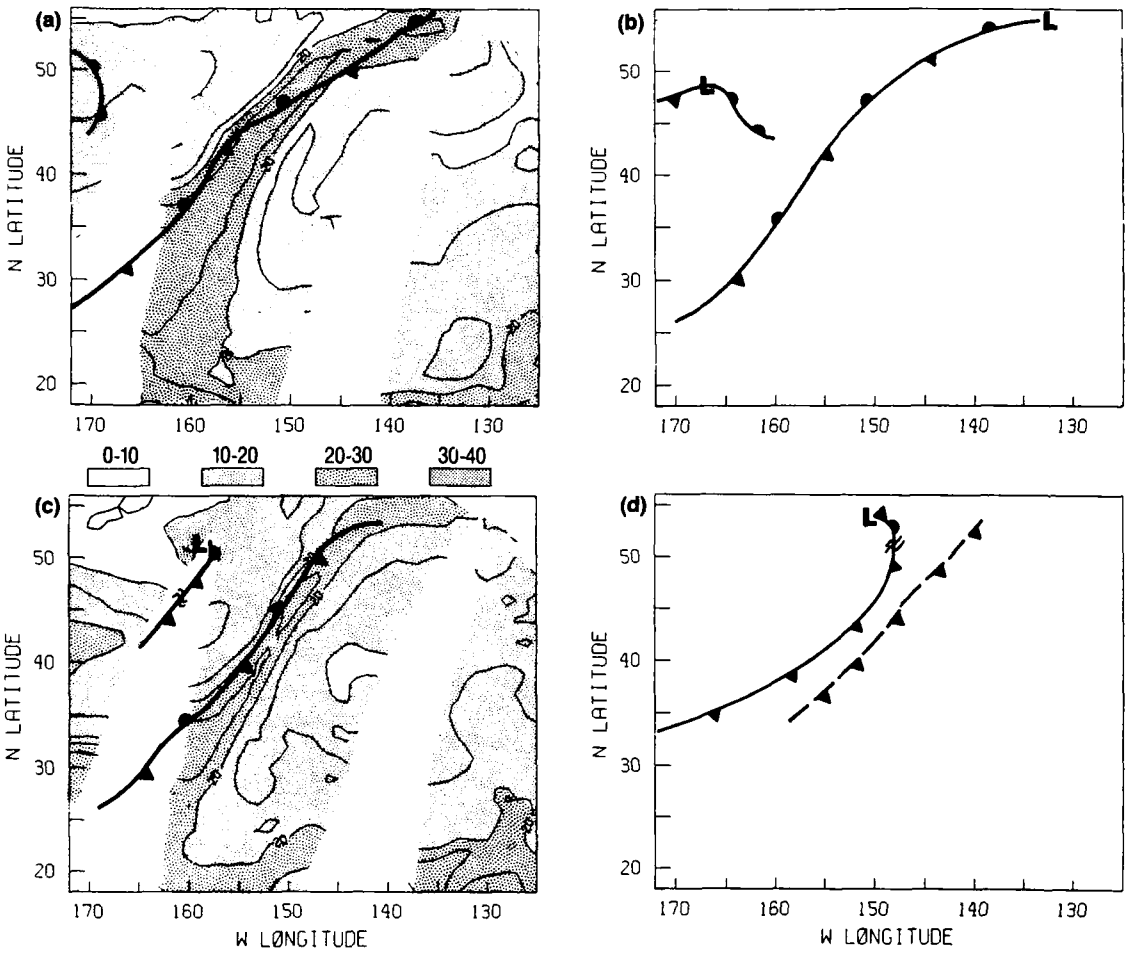

Fig. 13. Movement of atmospheric frontal systems as depicted by the NMC's surface pressure analyses. Background fields are SSM/I WV corrections from descending swaths on same day, contoured and shaded at 5-cm intervals. Darker shades represent higher WV content. (*a*) September 8, 1987, 0600 UT. (*b*) September 8, 1987, 1800 UT. (*c*) September 9, 1987, 0600 UT. (*d*) September 9, 1987, 1800 UT.

according to the distance over which the gradient strength was maintained, that is, the original measured distance. Table 3 illustrates that the majority of the WV correction gradients were sustained over 50 to 150 km, well within the range considered significant for ocean mesoscale features in the NEPAC region.

The final stage of the analysis is qualitative. Since the ultimate goal of the project is to use the altimeter data to locate the mesoscale ocean features, the impact of the wet tropospheric correction on the interpretation of the altimeter data is crucial. Thus each SSH residual track was subjectively analyzed to locate mesoscale fronts, which are generally characterized by a rise in the SSH residual proceeding from north to south along the altimeter track. Each apparent feature was noted, and the corrected and uncorrected SSH data along each track were compared. The observed differences in the apparent fronts were classified in one of three ways. If the feature was present in the original SSH data but not in the corrected data, then it was labeled a "false" signal. That is, the WV mimicked an ocean feature that was not really there. If the feature was not present in the original altimeter data but was identified in the corrected data, then it was classified as a "true ocean front" that was masked by the presence of atmospheric WV. If some hint of the feature was present initially and the feature was clearly identifiable in the corrected SSH data, then it was classified as an "enhanced" feature.

Of the 65 tracks processed, 31% contained false signals. At least one feature was completely masked by WV gradients in 35% of the tracks, and ocean signals were enhanced in 46% of the tracks (Table 4). When each feature was tallied individually, a total of 221 potential fronts were noted in the 65 tracks. Of these, approximately 128 features were not significantly contaminated by WV. However, 93 features (44% of the total) were interpreted differently as a result of making the wet tropospheric correction to the track. Of these, 22% were mimicked features, 28% were masked features, and 50% were enhanced features (Table 5). Thus if masking and enhancing are considered to be the same process and differ only in the magnitude of the change, then it appears that the obfuscation of the true ocean signal by the WV gradients is more of a problem than the so-called false signal, where the WV gradient is mistakenly interpreted as an ocean front or eddy.

Some studies [e.g., *Monaldo*, this issue] have been interested only in gradients that are equally as strong as the ocean signal. Thus the situation where the WV gradient is mimicking an ocean feature is of more concern. Masking of features is addressed only indirectly. That is, the WV correction gradient would have to occur at exactly the same strength

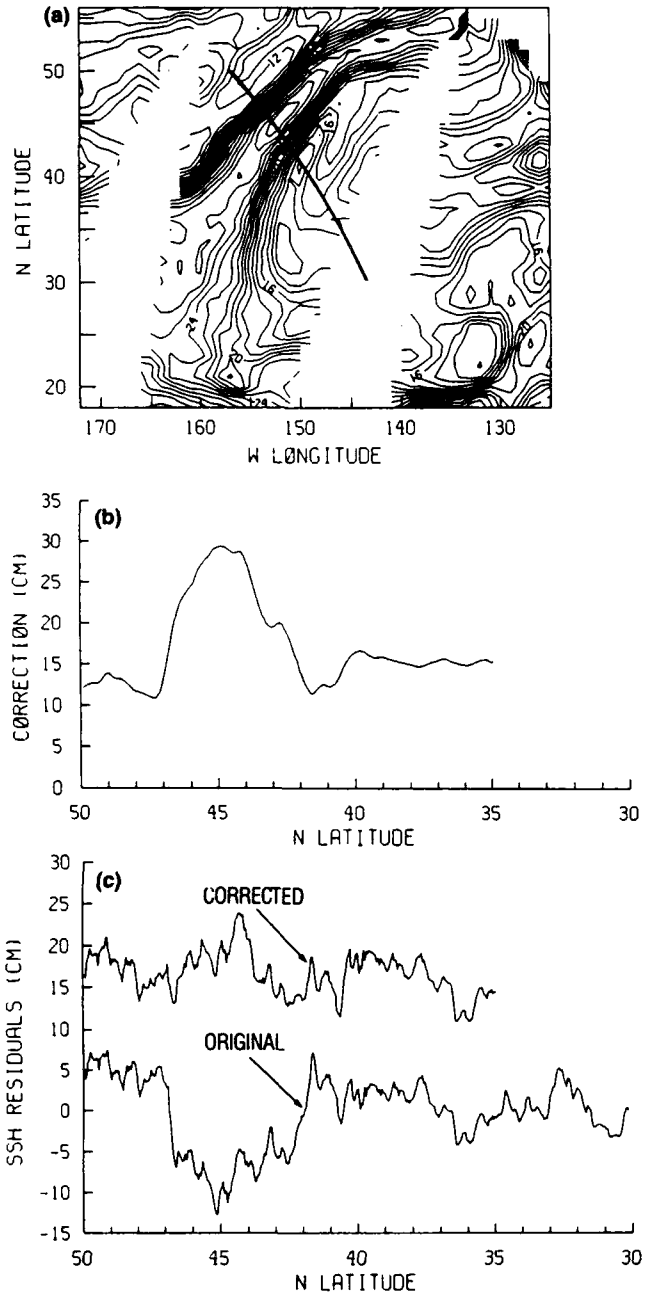

Fig. 14. WV correction applied to the 0700 UT Geosat track on September 8, 1987, using SSM/I data between 0400 and 0500 UT on the same day. (*a*) Two-dimensional correction field, contoured every 1 cm, showing the position of the track. (*b*) WV corrections (centimeters) analyzed along the track. (*c*) SSH residuals before and after the WV correction is made. The apparent ocean front at 42°N was largely induced by the WV.

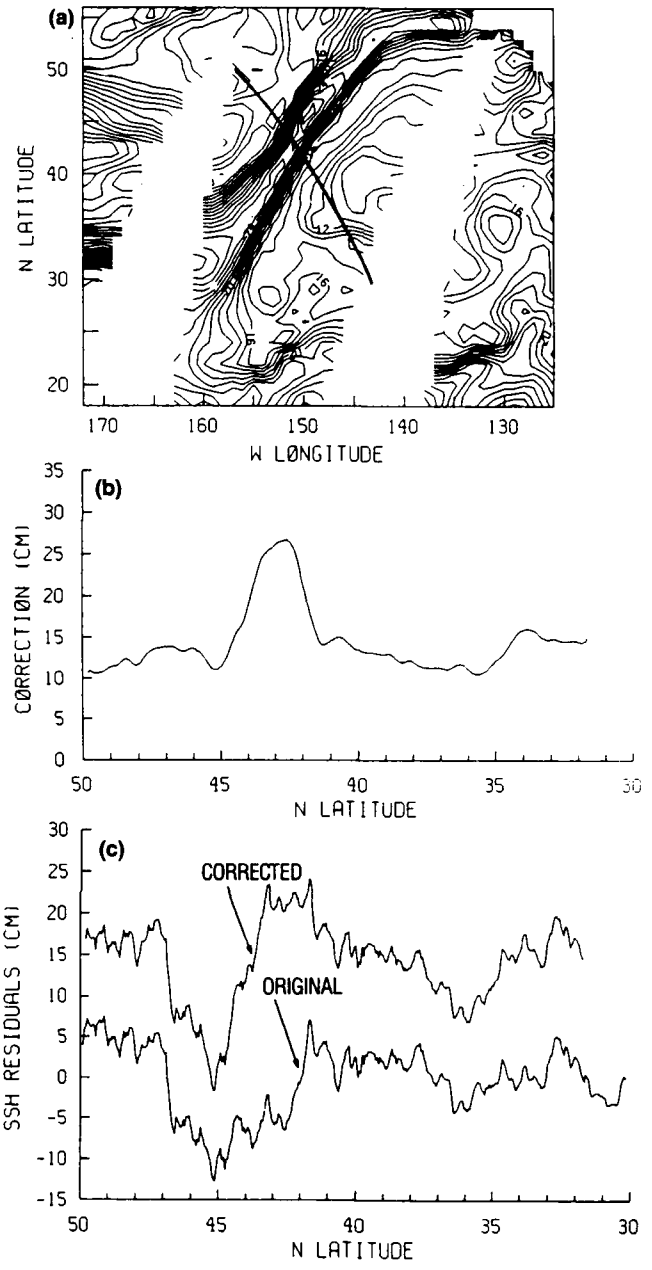

Fig. 15. WV correction applied to the same track as in Figure 14, but using SSM/I data between 0400 and 0500 UT on the next day, September 9, 1987. (*a*) Two-dimensional correction field, contoured every 1 cm, showing the position of the track. (*b*) WV corrections (centimeters) analyzed along the track. (*c*) SSH residuals before and after the WV correction is made. Notice how the corrected track differs from the one in Figure 14*c*. The WV data have induced a false ocean feature at 43°–45°N.

and at exactly the same location as the SSH gradient to be considered significant. Granted, the latter situation would happen infrequently. For example, in our study, if we compare the number of mimicked and masked features to the total number of 221 observed features, we find that WV gradients mimicked ocean SSH gradients in 9% of the cases, while features were masked 12% of the time. These figures indicate that significant gradients in the WV corrections were approximately colocated with the ocean frontal gradients about 20% of the time.

However, when we include not only the coincident situations but also those cases where the WV corrections modify the altimeter signal enough to alter the interpretation of the SSH data, the result is more far-reaching. Partly because we are using a fixed limit for determining the significant cases, features can be suppressed or enhanced by less than a 5-cm gradient in the WV correction. Thus changes in feature interpretation do not necessarily imply co-location of the strongest water vapor gradients with the strongest SSH gradients. Even an apparently insignificant WV correction

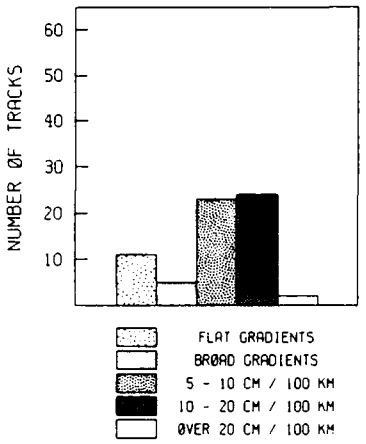

Fig. 16. Classification of the 65 total altimeter tracks into five categories based on the strength of the maximum WV correction gradient in the track. The number of tracks in each category is illustrated. The last three categories are considered significant, representing 75% of the total tracks.

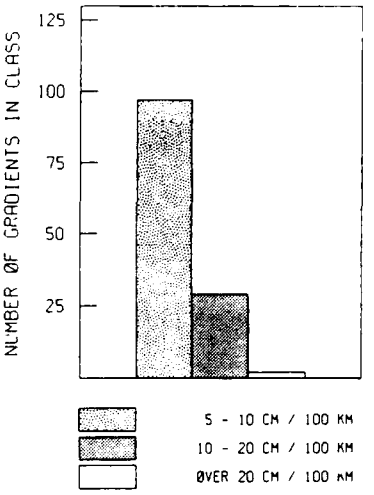

Fig. 17. Classification of the 128 significant WV correction gradients according to the gradient strength. The number of gradients measured in each class is illustrated.

gradient can alter feature identification. The large number of features affected by the WV is not surprising, considering that there are up to four weak ocean fronts in the NEPAC region, making it likely that at least one front will be affected by some portion of the atmospheric system.

CONCLUSIONS

Altimeter SSH data have proven to be a valuable tool for locating mesoscale fronts and eddies, particularly in western boundary current regimes where the SSH gradients are large. These data are especially useful when clouds inhibit the use of infrared imagery and when the ocean feature is submerged or does not have a strong SST signature. In the Geosat Exact Repeat Mission each location is viewed only once every 17 days. The distance between tracks is approximately 165 km at the equator. Thus for real-time oceanographic operations and applications, the information in each track is important. In an effort to extend the use of altimeter data to other areas where the SSH signal and variability are much lower, we have attempted to determine the importance of the wet tropospheric correction as a source of altimeter data error.

We used high-resolution (25 km) WV data from the DMSP SSM/I sensor to analyze WV correction fields for numerous Geosat tracks in the NEPAC region. This study is unique because it is the only work that has made time-coincident, wet tropospheric range corrections to actual SSH measurements along extended segments of altimeter tracks. The interpretation of the resulting differences clearly shows that in the NEPAC area the WV correction can significantly alter the apparent positions of the mesoscale ocean features in the altimeter data.

In the NEPAC region we found that the WV gradients associated with atmospheric frontal systems are comparable in strength to the signals of the ocean fronts in this area, where changes as small as 5–10 cm over 100 km are considered significant. What this implies, of course, is that the WV gradient may mimic or mask the mesoscale ocean features of interest. Thus the interpretation of the altimeter SSH data in this region is uncertain without the wet tropospheric correction. Even a 2- to 3-cm enhancement of the SSH gradient could mean the difference between locating or not locating a particular feature. The situation is further complicated by the number of weak oceanographic fronts in this area, making it more likely that the WV gradient will affect at least one of the fronts. It also appears that the ascending tracks are affected more often than the descending tracks, since the ascending tracks cross the normal southwest to northeast orientation of the atmospheric cold fronts.

We have shown that the timeliness of the data is critical. Because the atmospheric fronts and their associated WV fields may move rapidly through this area, blending data from multiple passes can oversmooth or offset the gradients in the water vapor field, reducing the true impact of the WV on the ocean signal. Using SSM/I data that are too far removed in time from the altimeter data can also introduce

TABLE 3. Sustained Strength of Significant Water Vapor Gradients

Gradient Magnitude, cm/100 km	Spatial Scale of the Measured Gradient									
	0–50 km		50–100 km		100–150 km		>150 km		Total	
	Number*	Percent†	Number*	Percent†	Number*	Percent†	Number*	Percent†	Number*	Percent†
5–10	6	6.2	41	42.3	40	41.2	10	10.3	97	100
10–20	4	13.8	9	31.0	12	41.4	4	13.8	29	100
≥20	0	0.0	1	50.0	0	0.0	1	50.0	2	100

*Out of 128 total measured gradients.
†In reference to the total number of gradients of this magnitude.

TABLE 4. Tracks with features Altered by Water Vapor

Type of Change	Number of Tracks*	Percent†
Enhanced features	30	46.2
Masked features	23	35.4
Mimicked features	20	30.8

*Out of 65 total tracks used for this study.
†In reference to total of 65 tracks.

false signals into the SSH data, which may be incorrectly interpreted as true ocean features. The scientific community would be best served by having a radiometer and an altimeter on the same satellite. With coincident measurements of WV and sea surface topography, we believe that the utilization of altimeter data can be extended to cases where the mesoscale ocean signals are weaker than those typically found in western boundary currents. The future European Remote Sensing Satellite (ERS-1) and Ocean Topography Experiment (TOPEX)/Poseidon altimeters both have boresighted radiometers that will permit this capability.

This study has concentrated on the NEPAC area, but the results shown here can likely be extended to other areas. Care must be taken, however, to assure that both the oceanographic and atmospheric conditions are similar; that is, the SSH gradients are weak and the atmospheric frontal systems are characterized by large air mass contrasts. Such areas might include, for instance, the north central and eastern Atlantic. A preliminary look at WV gradients in the northern Atlantic indicates that the wet tropospheric correction may be an unexpected source of error even at more northern latitudes [*May and Hawkins*, 1990]. But the relationship between the atmospheric and oceanographic conditions has been inadequately addressed in previous works. This question is particularly relevant in the *Bisagni* [1989] paper, since the study was limited to a small area in tropical latitudes east of a major continent.

Future work will pursue similar analyses for additional periods. This study concentrated on the month of September 1987, which is marked by strong air mass contrasts in the mid-latitudes. Data from other seasons may exhibit different properties. The winter season may be particularly interesting, as the capacity of the atmosphere to contain water vapor is diminished. Figure 18 illustrates a wintertime situation in the NEPAC sector. Note that significant gradients are still present in the WV correction field, even though the maximum is somewhat reduced and shifted southward from those seen during the summer-fall transition period. However, there is enough variability to encourage further study with a wintertime series of analyses.

TABLE 5. Ocean Features Altered by Water Vapor

Type of Change	Number of Features	Percent of Altered Features	Percent of Observed Features
Enhanced features	47	50.5	21.3
Masked features	26	28.0	11.8
Mimicked features	20	21.5	9.0
Total altered features	93	100.0	42.1
Total unaltered features	128		57.9
Total observed features	221		100.0

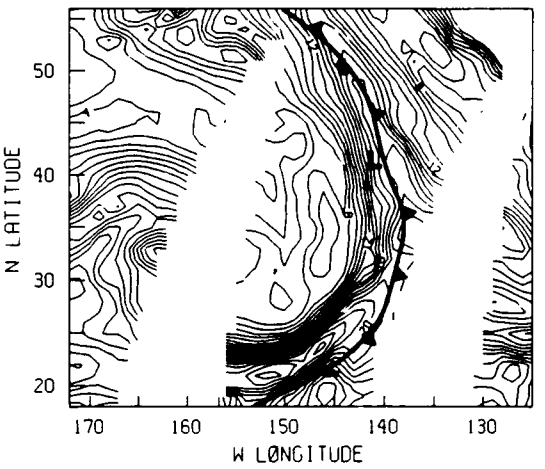

Fig. 18. Two-dimensional WV correction field analyzed using SSM/I data from 0200 UT to 0600 UT on February 23, 1988. The position of the atmospheric frontal system is valid at 1200 UT on the same day.

Since SSM/I WV data are the best available source for our current needs, more work needs to be done to evaluate their real potential. For example, we need to determine the temporal limits that should be placed on the use of SSM/I wet tropospheric corrections. These limits may be affected by the future launch of another DMSP platform with an SSM/I on board. Conceivably, data from two SSM/Is could be available as soon as spring 1990. For the NEPAC research project, we have implemented software to access the Fleet Numerical Oceanography Center SSM/I data base and make near-real-time corrections to the altimeter SSH residuals before the data are used for frontal analysis in the NEPAC area. However, this solution is not fully satisfactory. Since we to not feel justified using WV data that are more than a few hours removed from the altimeter data, large portions of the tracks cannot be corrected.

We have made several assumptions in our data processing, which may or may not affect our conclusions. First, we have assumed that the formation of SSH residuals by subtracting a mean surface does not consistently reduce the signal of the mesoscale ocean features beyond detection. While the mean surface typically contains longer wavelengths, this assumption may not be valid for each individual case. Furthermore, we believe the objective techniques used to smooth and analyze both the altimeter SSH residuals and the SSM/I WV measurements reduce the random noise present in the original data while still showing the signals of interest. Thus our interpretations assume that the analyzed data accurately represent the physical phenomena. Finally, we are looking for ocean signals that are near the noise level of the altimeter. While we know that such weak features are present, we acknowledge that we are pushing the generally accepted limits of ocean feature detection.

These things considered, we still feel that the presence of WV is a serious hindrance to the use of altimeter data for mesoscale feature detection in areas where the ocean signal is weak and the SSH variability is low. We have shown that the wet tropospheric correction dramatically alters the appearance of the SSH residuals along Geosat tracks in the NEPAC region. While we have not shown that the corrected data are any more accurate than the uncorrected data,

intuition tells us that removing a known source of error from the original measurements will result in a more accurate product. Thus we leave it to a future study to make use of independent data sources, such as recently gathered bathythermograph measurements, to perform an extensive verification of the frontal positions in the corrected tracks.

Acknowledgments. Many people have contributed their time and ideas to this project. The SSM/I geophysical data were processed by Frank Wentz of Remote Sensing Systems, Santa Rosa, California. The SSM/I water vapor corrections were computed locally from the Wentz data by Nita Chase of NORDA and by Fred Abell, Sylvia Seal, and Bobby Grant of Sverdrup Technology. The Geosat altimeter data were processed by Conrad Johnson, NORDA, and Natalie Koennen, Sverdrup Technology. We must recognize our colleagues who have participated in the GOAP and NEPAC remote sensing efforts: Jim Mitchell, Matt Lybanon, and Doug May. Finally, we would like to thank Richard Crout of Planning Systems, Incorporated, for providing us with the benefit of his experience in analyzing altimeter data and for assisting in interpretating of the NEPAC altimeter SSH residuals. This work was supported by the Chief of Naval Operations (OP-096) and the Naval Space and Warfare Command under program element 63704N, Satellite Applications and Techniques (SAAT), A. E. Pressman, Program Manager. NOARL contribution JA 321:044:89. NORDA is now known as the Naval Oceanographic and Atmospheric Research Laboratory. This document has been reviewed and is approved for public release.

REFERENCES

Alishouse, J., S. Synder, J. Vongsathorn, and R. Ferraro, Determination of oceanic total precipitable water from the SSM/I, *IEEE J. Geosci. Remote Sens.*, in press, 1990.

Askne, J., G. Elgered, and H. Nordius, Atmospheric water vapour corrections for altimetry measurements, Proceedings of the International Geoscience and Remote Sensing Symposium, 1986, *Eur. Space Agency Spec. Publ., ESA SP-254*, vol. 3, 1543–1548, 1986.

Bernstein, R., G. Born, and R. Whritner, Seasat altimeter determination of ocean current variability, *J. Geophys. Res.*, *87*, 3261–3268, 1982.

Bisagni, J., Wet tropospheric range corrections for satellite altimeter–derived dynamic topographies in the western North Atlantic, *J. Geophys. Res.*, *94*, 3247–3254, 1989.

Bjerknes, J., On the structure of moving cyclones, *Geofys. Publ.*, *1*(2), 1–8, 1919.

Chang, H., T. Wilheit, and P. Gloersen, Global maps of atmospheric water vapor, cloud water, and rainfall derived from Nimbus-7 scanning multichannel microwave radiometer data: A case study, in *Proceedings, Oceanography From Space Symposium*, pp. 683–689, Plenum, New York, 1980.

Chang, H., P. Hwang, T. Wilheit, A. Chang, D. Staelin, and P. Rosenkranz, Monthly distributions of precipitable water from the Nimbus 7 SMMR data *J. Geophys. Res.*, *89*, 5328–5334, 1984.

Chelton, D., K. Hussey, and M. Parke, Global satellite measurements of water vapour, wind speed and wave height, *Nature*, *294*, 529–532, 1981.

Cheney, R., Comparison data for Seasat altimetry in the western North Atlantic, *J. Geophys. Res.*, *87*, 3247–3253, 1982.

Cressman, G., An operational objective analysis system, *Mon. Weather Rev.*, *87*, 367–374, 1959.

DiMego, G., The National Meteorological Center regional analysis system, *Mon. Weather Rev.*, *116*, 977–1000, 1989.

Hawkins, J., and P. Smith, Effects of atmospheric water vapor on the detection of mesoscale oceanographic features from Geosat, *NORDA Rep. 126*, 21 pp., Nav. Ocean Res. and Develop. Activ., Stennis Space Center, Miss., 1986.

Hollinger, J., DMSP special sensor microwave/imager calibration/validation, final report, 158 pp., Nav. Res. Lab., Washington, D. C., 1989.

Katsaros, K., and R. Lewis, Mesoscale and synoptic scale features of North Pacific weather systems observed with the scanning multichannel microwave radiometer on Nimbus 7, *J. Geophys. Res.*, *91*, 2321–2330, 1986.

Lipes, R., Description of Seasat radiometer status and results, *J. Geophys. Res.*, *87*, 3385–3395, 1982.

Lybanon, M., and R. Crout, The NORDA Geosat ocean applications program, *Johns Hopkins APL Tech. Dig.*, *8*(2), 212–218, 1987.

May, D., and J. Hawkins, Altimeter height corrections due to atmospheric water vapor in the Greenland–Iceland–United Kingdom (GIUK) gap (abstract), *Eos Trans. AGU*, *71*, 127, 1990.

McConathy, D., and C. Kilgus, The Navy Geosat mission: An overview, *Johns Hopkins APL Tech. Dig.*, *8*(2), 170–175, 1987.

McMurdie, L., and K. Katsaros, Atmospheric water distribution in a mid-latitude cyclone observed by the Seasat scanning multichannel microwave radiometer, *Mon. Weather Rev.*, *113*, 584–598, 1985.

McMurdie, L., G. Levy, and K. Katsaros, On the relationship between scatterometer-derived convergences and atmospheric moisture, *Mon. Weather Rev.*, *115*, 1281–1294, 1987.

Menard, Y., Observations of eddy fields in the northwest Atlantic and northwest Pacific by Seasat altimeter data, *J. Geophys. Res.*, *88*, 1853–1866, 1983.

Monaldo, F., Path length variations caused by atmospheric water vapor and their effects on the measurement of mesoscale ocean circulation features by a radar altimeter, *J. Geophys. Res.*, this issue.

Njoku, E., and L. Swanson, Global measurements of sea surface temperature, wind speed and atmospheric water content from satellite microwave radiometry, *Mon. Weather Rev.*, *111*, 1977–1987, 1983.

Phoebus, P., and J. Hawkins, The use of SSM/I water vapor data to correct altimeter sea surface height measurements (abstract), *Eos Trans. AGU*, *69*, 1281, 1988.

Roden, G., On long wave disturbances of dynamic height in the North Pacific, *J. Phys. Oceanogr.*, *7*, 41–49, 1977.

Roden, G., and A. Robinson, Subarctic frontal zone in the northeastern Pacific: Mesoscale structure and synoptic description, *Rep. in Meteorol. and Oceanogr. 31*, 71 pp. Div. of Appl. Sci., Harvard Univ., Cambridge, Mass., 1988.

Saastamoinen, J., Atmospheric correction for troposphere and stratosphere in radio ranging of satellites, in *The Use of Artificial Satellites for Geodesy*, *Geophys. Monogr. Ser.*, vol. 15, edited by S. W. Henriksen, A. Mancini, and B. H. Chovitz, pp. 247–251, AGU, Washington, D. C., 1972.

Sailor, R., and A. LeSchack, Preliminary determination of the Geosat radar altimeter noise spectrum, *Johns Hopkins APL Tech. Dig.*, *8*(2), 182–183, 1987.

Short, D., and C. Prabhakara, Satellite derived atmosphere water vapor as a tracer of large scale interactions between the atmosphere and ocean, in *Proceedings Satellite/Remote Sensing and Applications Conference*, pp. 143–148, American Meteorological Society, Boston, Mass., 1984.

Staelin, D., K. Kunzi, R. Pettyjohn, R. Poon, R. Wilcox, and J. Waters, Remote sensing of atmospheric water vapor and liquid water with the Nimbus 5 microwave spectrometer, *J. Appl. Meteor.*, 15, 1204–1214, 1976.

Tapley, B., J. Lundberg, and G. Born, The Seasat altimeter wet tropospheric range correction, *J. Geophys. Res.*, *87*, 3213–3220, 1982.

Tapley, B., J. Lundberg, and G. Born, The Seasat altimeter wet tropospheric range correction revisited, *Mar. Geod.*, *8*, 221–248, 1984.

Taylor, P., K. Katsaros, and R. Lipes, Determinations by Seasat of atmospheric water and synoptic fronts, *Nature*, *294*, 737–739, 1981.

Thompson, J., G. Born, and G. Maul, Collinear-track altimetry in the Gulf of Mexico from Seasat: Measurements, models, and surface truth, *J. Geophys. Res.*, *88*, 1625–1636, 1983.

J. D. Hawkins, Naval Oceanographic and Atmospheric Research Laboratory, Ocean Sensing and Prediction Division, Stennis Space Center, MS 39529.

P. A. Phoebus, Naval Oceanographic and Atmospheric Research Laboratory, Atmospheric Directorate, Monterey, CA 93943.

(Received May 31, 1989;
accepted July 28, 1989.)

REPORT DOCUMENTATION PAGE

Form Approved
OMB No. 0704-0188

1. Agency Use Only *(Leave blank).*

2. Report Date. March 1990

3. Report Type and Dates Covered.

4. Title and Subtitle.
The Impact of the Wet Tropospheric Correction on the Interpretation of Altimeter-Derived Ocean Topography in the Northeast Pacific

5. Funding Numbers.
Program Element No. 63704N
Project No. 0101
Task No. 100
Accession No. DN394421

6. Author(s).
Patricia A. Phoebus and Jeffrey D. Hawkins

7. Performing Organization Name(s) and Address(es).
NOARL
CODE 321
SSC, MS 39529-5004

8. Performing Organization Report Number.
JA 321:044:89

9. Sponsoring/Monitoring Agency Name(s) and Address(es).
Sapce and Naval Warfare Systems Command
PMW-141
Washington, DC

10. Sponsoring/Monitoring Agency Report Number.

11. Supplementary Notes.

12a. Distribution/Availability Statement.
Approved for public release; distribution is unlimited.

12b. Distribution Code.

13. Abstract *(Maximum 200 words).*

Atmospheric water vapor data derived from the special sensor microwave/imager (SSM/I) are used to make time-coincident, wet tropospheric range corrections to Geosat altimeter data in the northeast Pacific. The original and corrected sea surface height residuals along numerous tracks are examined to determine the impact of water vapor on the altimeter signal. Mesoscale feature analyses of corrected and uncorrected altimeter data are used to assess the impact of water vapor path lengthening in areas of low sea surface height variability. Results indicate that the horizontal spatial variations in the water vapor height corrections are frequently similar to true oceanographic gradients. Interpretation of altimeter data is affected in several ways. The unaccounted for presence of atmospheric water vapor may mimic or mask the true ocean features, and even small changes in the water vapor over short spatial scales can enhance a partially abscured feature. Analyses of all Geosat tracks crossing the area of interest in September 1987 clearly illustrate that water vapor frequently contaminates the ocean topography measurements, making the water vapor adjustment critical before the altimeter data can be successfully used

14. Subject Terms.
(U) SSM/I, (U) Passive Microwave, (U) Sea Ice

15. Number of Pages. 13

16. Price Code.

17. Security Classification of Report.	18. Security Classification of This Page.	19. Security Classification of Abstract.	20. Limitation of Abstract.
Unclassified	Unclassified	Unclassified	SAR

13. Abstract

to locate and identify mesoscale ocean features. Futhermore, the SSM/I and Geosat data must be closely matched in both space and time, a difficult task since it takes 3.5 days to obtain global SSM/I coverage with one operational sensor. To optimize the mesoscale oceanographic application of altimeter data, a bore-sighted radiometer should be included on all altimeter spaceborne platforms.